Microb Ecol
DOI 10.1007/s00248-016-0777-x

ENVIRONMENTAL MICROBIOLOGY

Deciphering the Pathobiome: Intra- and Interkingdom Interactions Involving the Pathogen *Erysiphe alphitoides*

Boris Jakuschkin[1] · **Virgil Fievet**[1] · **Loïc Schwaller**[2,3] · **Thomas Fort**[1] · **Cécile Robin**[1] · **Corinne Vacher**[1]

Received: 2 March 2015 / Accepted: 21 April 2016

Abstract Plant-inhabiting microorganisms interact directly with each other, forming complex microbial interaction networks. These interactions can either prevent or facilitate the establishment of new microbial species, such as a pathogen infecting the plant. Here, our aim was to identify the most likely interactions between *Erysiphe alphitoides*, the causal agent of oak powdery mildew, and other foliar microorganisms of pedunculate oak (*Quercus robur* L.). We combined metabarcoding techniques and a Bayesian method of network inference to decipher these interactions. Our results indicate that infection with *E. alphitoides* is accompanied by significant changes in the composition of the foliar fungal and bacterial communities. They also highlight 13 fungal operational taxonomic units (OTUs) and 13 bacterial OTUs likely to interact directly with *E. alphitoides*. Half of these OTUs, including the fungal endophytes *Mycosphaerella punctiformis* and *Monochaetia kansensis*, could be antagonists of *E. alphitoides* according to the inferred microbial network. Further studies will be required to validate these potential interactions experimentally. Overall, we showed that a combination of metabarcoding and network inference, by highlighting potential antagonists of pathogen species, could potentially improve the biological control of plant diseases.

Keywords Plant microbiota · Plant-pathogen interaction · Pathobiome · Microbial network · Network inference · Disease resistance · Biocontrol · Powdery mildew

Introduction

Almost all plant tissues host a microbial community [1]. These microbes interact with each other directly through pairwise ecological interactions such as predation, parasitism, mutualism, or competition [2]. The interactions can involve microorganisms belonging to the same kingdom or different kingdoms [3]. They can involve plant-beneficial microorganisms as well as plant pathogens [4]. The notion that the pathogens live and interact with other microorganisms has recently led to the development of the "pathobiome" concept, in which the pathogenic agent is integrated into its biotic environment [5]. Elucidation of the components of the pathobiome is a prerequisite for understanding the pathogenesis, persistence, transmission, and evolution of pathogenic agents [5]. Pathobiome studies will lead to new approaches to plant protection, paralleling those currently being developed for the study of human diseases [6]. The role of the commensal flora in animal health is, indeed, well recognized [7], and its manipulation to treat human diseases is a highly promising and competitive field of current medical research [8, 9]. Similar approaches should be considered to improve plant health [10, 11]. A current challenge is therefore to decipher the interactions between plant pathogens and the resident microbial community to better understand the mechanisms of plant disease resistance and to improve methods of biological control [12, 13].

Electronic supplementary material The online version of this article (doi:10.1007/s00248-016-0777-x) contains supplementary material, which is available to authorized users.

✉ Corinne Vacher
corinne.vacher@pierroton.inra.fr

[1] BIOGECO, INRA, University of Bordeaux, F-33615 Bordeaux, Pessac, France

[2] AgroParisTech, UMR 518 MIA, F-75005 Paris, France

[3] INRA, UMR 518 MIA, F-75005 Paris, France

Published online: 05 May 2016

Ecological networks are now the standard method for representing and analyzing direct interactions between species. Network architecture governs the stability of ecological communities [14, 15], including their invasibility by new species [16]. In the case of microbial communities, networks often represent associations between species rather than interactions. Microbial association networks typically contain positive links (indicating species co-occurrence) and negative links (indicating co-exclusion). These associations can arise from direct interactions between species. A positive association between two species can, for instance, reveal a mutualistic interaction, while a negative association can arise from competition. Alternatively, associations can reflect indirect interactions between species (i.e., mediated by a shared interacting partner), or shared environmental requirements [12]. Several methods have been developed to detect associations between microbial species from metabarcoding datasets [2, 12, 17–19], but there is no standard method for highlighting direct ecological interactions.

In the present study, we used a Bayesian method of network inference [20, 21] to decipher the pathobiome of *Erysiphe alphitoides*, the causal agent of oak powdery mildew [22, 23]. This fungus, which covers oak leaves with spots or patches of white mycelium and spores, causes one of the most common diseases in European forests [22]. Like most powdery mildews, *E. alphitoides* grows superficially on leaves, sometimes covering up to 80 % of the upper leaf surface, whilst obtaining resources from leaf cells via haustoria [24]. *E. alphitoides* interacts directly with certain foliar microorganisms, such as the mycoparasites of the genus *Ampelomyces* [25]. It can also interact indirectly with other microorganisms by altering the chemistry and physiology of oak leaves [26, 27]. Our aim here was to better understand the relationships between the fungal pathogen *E. alphitoides* and other foliar microorganisms of oak (*Quercus robur* L.), including both epiphytes and endophytes. We specifically addressed the following questions: (1) Is infection with *E. alphitoides* accompanied by changes in the composition of the foliar microbial community? (2) Which microbial species are the most likely to interact directly with *E. alphitoides*?

Materials and Methods

Study Site and Sampling Design

We sampled three trees with different levels of susceptibility to the pathogen, in order to obtain a gradient of infection levels. The three trees belonged to a full-sib family of *Q. robur* L. planted for a field experiment established in 2000 at INRA-Bourran, in South West France (44.20° N, 0.24° W) [28]. They were located within 5 m of each other. They were previously characterized as highly susceptible, intermediately resistant, and strongly resistant to powdery mildew on the basis of 5 years of visual observations (Desprez-Loustau M-L, personal communication).

On July 29th 2011, we collected 40 leaves per tree: 10 leaves from each of four branches at an approximate height of 2 m. The leaves chosen were evenly spaced between the trunk and the tip of the branch. We collected leaves strictly from the first flush. We measured the level of powdery mildew infection as the proportion of the upper leaf area displaying symptoms. We also determined the position of each leaf within the canopy: its distance to the ground, to the base of the branch, to the tree trunk, and the orientation of the branch (South-West versus North-East). Each leaf was then cut at the base of the petiole and placed in a sterile bag containing silica gel. The bags, which were hermetically sealed, were then stored in the dark at +18 °C in the laboratory. A preliminary experiment had been performed previously to assess the effect of storing oak leaves in silica gel on the composition of the fungal community inferred by 454 pyrosequencing. We found no significant difference between the communities of fresh leaves and those of leaves stored in silica gel (Methods S1).

Leaf DNA Extraction

Leaf DNA extraction was performed 3 months after sampling. We prepared the leaf material for DNA extraction in a laminar flow hood. Sample contamination was prevented by disinfecting the hood and all tools with sodium hypochlorite followed by 70 % ethanol and then exposing them to UV light for 40 min. Plastic ware and tungsten carbide beads were autoclaved for 2 h before use. Similarly, the tools used for leaf handling were sterilized before each use, by dipping in 70 % alcohol and flaming over an electric Bunsen burner. We used a metal corer to excise two 0.5-cm^2 discs from each side of the middle leaf vein. The four discs were evenly distributed over the leaf, and their positions were selected at random, without consideration of any visible symptoms of *E. alphitoides* infection. The four discs were then placed in a collection microtube (QIAGEN DNeasy® 96 Plant Kit) containing one tungsten carbide bead. We used Geno/Grinder® (SPEX SamplePrep, Metuchen, NJ, USA) to homogenize the leaf material, at 1600 strokes per minute for 90 s. Homogenized samples were stored at −80 °C overnight. We used the QIAGEN DNeasy 96 Plant Kit to extract the DNA (following the protocol for frozen plant tissue). We determined the DNA concentration with NanoDrop 8000 and diluted all DNA working solutions to 1 ng μl^{-1}.

Amplification and Sequencing of the Fungal Assemblages

We used the rapidly evolving internal transcribed spacer 1 (ITS1) as the DNA metabarcoding marker for fungi [29].

We used titanium fusion primers for the PCR amplification, as follows. The forward primers were composed of the 454 A-adaptor, a sample-specific 6-bp tag, and the ITS1F primer [30]. The reverse primer consisted of the B-adaptor and the ITS2 primer [31] (Tab. S1). The PCR mixture (50 μl) contained 2.5 units of Silverstar *Taq* polymerase (Eurogentec), 5 μl of the 10× PCR buffer supplied by the manufacturer, 2 μl $MgCl_2$ (50 mM), 2 μl dNTPs (5 mM), 1 μl of each primer (10 μM), 0.5 μl of 100 mg ml^{-1} BSA, and 5 ng DNA template. PCR was carried out as follows: an initial phase at 95 °C (5 min), followed by 35 cycles of 95 °C (30 s), 54 °C (60 s), and 72 °C (90 s) and a final step at 72 °C (10 min). Samples were amplified in triplicate and pooled for purification with AMPure magnetic beads (Beckman Coulter Genomics, Danvers, MA, USA). DNA concentration was determined with a NanoDrop 8000, and the samples were pooled in equimolar ratios to obtain the amplicon libraries. We used 40 tags in total, generating one amplicon library per tree. The libraries were sequenced in separate 1/8th runs on a 454 GS Junior sequencer (454 Life Sciences, Branford, CT, USA) at the *Centre de Génomique Fonctionnelle de Bordeaux* (CGFB, Bordeaux, France). Sequencing was unidirectional and started with the A adaptor. The 454 sff files are available from the European Nucleotide Archive (http://www.ebi.ac.uk/ena/data/view/PRJEB7319).

Amplification and Sequencing of the Bacterial Assemblages

We applied the microbiome profiling method developed by Gloor et al. [32], which uses combinatorial sequence tags attached to PCR primers to amplify the hypervariable V6 region of the 16S rRNA gene [33]. This tagging, together with the Illumina paired-end protocol, made it possible to examine hundreds of samples with far fewer primers (Tab. S2) than would be required if the tags were incorporated at only one end. The PCR mixture (50 μl) contained 2.5 units of Silverstar *Taq* polymerase (Eurogentec), 5 μl of the 10× PCR buffer supplied by the manufacturer, 2 μl $MgCl_2$ (50 mM), 2 μl dNTPs (5 mM), 1 μl of 10 μM forward primer, 1 μl of 10 μM reverse primer, 0.5 μl of 100 mg ml^{-1} BSA, and 5 ng DNA template. PCR was carried out as follows: an initial phase at 95 °C (2 min), followed by 30 cycles of 95 °C (30 s), 56 °C (30 s), and 72 °C (30 s) and a final extension at 72 °C (5 min). Samples were amplified in triplicate and pooled for purification with AMPure magnetic beads (Beckman Coulter Genomics, Danvers, MA, USA). We quantified the PCR products with the Nanodrop 8000 and pooled them at equimolar ratios. The final DNA library was sequenced on the Illumina platform GAIIx at the *Centre de Génomique Fonctionnelle de Bordeaux* (CGFB, Bordeaux, France). The fastq files are available from the European Nucleotide Archive (http://www.ebi.ac.uk/ena/data/view/PRJEB7319).

Processing of the Fungal 454 Pyrosequencing Data

We used QIIME v.1.7.0 [34] for quality filtering, demultiplexing, and noise reduction. After the removal of tags and primers, all sequences shorter than 100 nucleotides were discarded. Quality filtering was achieved with a sliding window test for quality scores, with a window size of 50 nucleotides and a minimum quality score of 25. The sequences were truncated at the beginning of the poor-quality window and tested for the minimum sequence length of 100 nucleotides. The highly conserved ribosomal genes flanking the ITS1 marker may distort sequence clustering and similarity searches. We therefore removed them from the dataset with Fungal ITS Extractor 1.1 [35]. ITS1 sequences shorter than 100 nucleotides were discarded, and sequences longer than 280 nucleotides were trimmed at the 3′-end. Before the clustering step, we combined the dataset with a larger, unpublished 454 fungal dataset acquired by sampling leaves from other oak trees, to reduce the number of singletons. We discarded singleton reads before clustering to minimize spurious operational taxonomic unit (OTU) identifications.

OTUs were clustered with UPARSE-OTU [36], an algorithm implemented within Usearch v.7 [37] that simultaneously performs chimera filtering and OTU clustering. This algorithm identifies a set of OTU representative sequences at the 97 % sequence similarity threshold, corresponding roughly to the difference at species level [38]. Unfortunately, other *Erysiphe* species, such as *Erysiphe quercicola* and *Erysiphe hypophylla*, have an ITS sequence differing from that of *E. alphitoides* by less than 3 % [22]. The ITS sequences of these species therefore cluster together when a 97 % similarity threshold is used. We overcame this problem by performing a BLAST search of all sequences against a custom-made taxonomic database of the genus *Erysiphe*. Before OTU clustering with UPARSE-OTU, we extracted all sequences with successful hits against *E. alphitoides* into a separate file and assigned the corresponding read counts.

All fungal OTUs were then taxonomically assigned by performing by BLAST searches against the Fungal ITS Database [39] (as of March 15, 2012). We modified the taxonomic file associated with this database to equalize the length of taxonomic ranks using the NCBI Taxonomy Browser. We also corrected a few incorrect taxonomic assignments in the case of *Erysiphe* species and removed a few non-fungal sequences. We used this database to assign a taxon to the most abundant sequence of each OTU, using QIIME (v.1.7.0) with standard settings (BLAST searches, e-value: 0.001, minimum percent identity: 90). We also compared the representative sequence of each OTU with the sequences deposited in GenBank, using the BLASTn algorithm [40], to exclude possible *Q. robur* sequences and to carefully check the taxonomic assignments of the fungal OTUs associated to *E. alphitoides*. These latter were also compared to the taxonomic assignments

obtained from the RDP Classifier [41] using the UNITE Fungal ITS Trainset (July 4, 2014) as a reference database [42].

Processing of the Bacterial Illumina Solexa Data

We assembled the paired-end reads with PANDAseq [43]. Reads were then demultiplexed as described by Gloor et al. [32], with a custom Bash shell script. We removed oak chloroplast sequences before clustering. OTUs were then clustered as described for fungi. The origin of the OTU representative sequences (archaeal, bacterial, nuclear eukaryote, mitochondrial, or chloroplast origin) was determined with Metaxa [44], and we retained only the bacterial OTUs. Taxonomic assignments of all bacterial OTUs were performed with the RDP Classifier program (v.2.5) [41], as implemented in QIIME (v.1.7.0), with standard settings and Greengenes 13_5 as the reference sequences. The taxonomic assignments of the bacterial OTUs associated to *E. alphitoides* were moreover carefully checked by BLASTn against GenBank [40], and by using the RDP Classifier [41] with the 16s rRNA training set 14 (May 2015) as a reference database [42].

Comparison of Infection Levels Between Trees

All statistical analyses were performed in R [45]. We first verified that the three trees differed in their level of susceptibility to *E. alphitoides*. The effect of tree on the percentage of the upper leaf area displaying symptoms (arc-sine transformed) was assessed with a generalized linear model (GLM) with a Gaussian distribution. A second model was built to assess differences in the number of *E. alphitoides* reads between trees. We did not rarefy the data [46] but rather took into account the total number of reads per sample (log-transformed) as an offset. We controlled for overdispersion by using a negative binomial generalized linear model (NBGLM).

Relationship Between the Level of Infection with *E. alphitoides* and the Composition of Foliar Microbial Communities

All analyses described hereafter were performed on the data for the susceptible tree. We first investigated whether the number of reads assigned to *E. alphitoides* could be used as a proxy for the level of infection, by testing the effect of the percentage of the upper leaf area displaying symptoms on the number of *E. alphitoides* reads, using a NBGLM. The total number of reads per sample (log-transformed) was included as an offset.

We then investigated the relationship between the level of infection with *E. alphitoides* and the composition of foliar microbial communities. We used principle coordinates analyses (PCoA) on rarefied datasets to visualize differences in microbial community composition between leaves. Compositional dissimilarities between leaves were assessed using the Bray-Curtis index. The rarefaction threshold was 1226 reads for fungal data and 114 reads for bacterial data. The reads assigned to *E. alphitoides* were not included in the fungal dataset because they were used as an explanatory variable for variations in fungal community composition. We strengthened the robustness of our results to rarefaction, by performing 100 rarefactions, followed by 100 PCoAs. We calculated the mean and the standard error of the mean for the coordinates of the samples on the first two axes of the PCoA. The mean coordinates on the first two axes (*comp1* and *comp2*, respectively) were used as proxies for microbial community composition. The effect of the percentage of *E. alphitoides* reads on these two variables was investigated with a GLM with a Gaussian distribution.

We finally investigated the associations between microbial OTUs and leaf type (highly infected with *E. alphitoides versus* "uninfected"), using the point biserial correlation coefficient. A leaf was considered to be highly infected if the percentage of reads assigned to *E. alphitoides* exceeded 5 %. Associations between OTUs and leaf type were calculated for all OTUs accounting for more than 0.5 % of the sequences for the tree susceptible to *E. alphitoides*.

Statistical Inference of the Putative Direct Interactions Between *E. alphitoides* and Other Members of the Foliar Community

A previous study [12] has revealed a very high number of microbial associations within foliar microbial communities of oak. Here, we attempted to remove associations due to shared environmental requirements (e.g., two OTUs are associated because both are adapted to shade leaves) and shared interacting partners (e.g., two OTUs are associated because both are parasites of a third OTU). We highlighted the most likely interactions between *E. alphitoides* and other foliar microorganisms, by constructing a microbial network having OTUs as nodes and putative direct interactions between OTUs as edges. Network construction was based on a subset of the most abundant OTUs: 48 bacterial OTUs and 66 fungal OTUs (including *E. alphitoides*). Each represented at least 0.5 % of the sequences for at least one of the three trees.

We first attempted to remove associations due to shared environmental requirements by fitting the number of reads for each OTU using NBGLMs with environmental variables as predictors and the total number of reads per sample (log-transformed) as an offset. GLMs with a Poisson distribution were used for a few OTUs. The position of a leaf within the canopy was taken as a proxy for its abiotic environment (e.g., temperature, UV exposure). The four variables describing the position of the sampled leaves—their distances to the ground,

to the base of the branch, and to the tree trunk, and the orientation of the branch—were included in the GLM as single predictive factors. The Pearson residuals obtained from the fitted models were used to model the dependence structure between the OTUs, using Gaussian copulas.

We then attempted to remove associations due to shared interacting partners, by using the Bayesian network inference method [20] implemented in the R package *saturnin* [21]. The method considered a class of acyclic unidirectional networks (called spanning trees) to explain the dependence structure between the OTUs. Direct edges between OTUs were obtained by averaging (in an exhaustive manner) over these simple networks, thus counterbalancing their individual simplicity. This averaging can result in cycles or disconnected OTUs in the inferred network. The inferred network therefore had OTUs as nodes, and only direct dependencies between OTUs as edges. The inference yielded, for any possible edge, the probability of its belonging to the true network. The prior probability of interactions was fixed at 0.5. Only edges with an apparent posterior probability greater than 0.5 were retained in the interaction network. The sign of the interactions was determined from the sign of the *a posteriori* maximum of the correlation in the associated bivariate Gaussian copula.

The inferred microbial network had positive and negative edges, which were visualized with Gephi (v. 0.8.2 beta) software [47]. Based on the theoretical outcome of each type of interaction for each interacting partner (positive (+), negative (−) or null (0); see [2]), positive edges may indicate mutualism (+/+) or commensalism (+/0). Negative edges may indicate competition (−/−) or amensalism (−/0). The correspondence between network edges and parasitism or predation (+/−) is less straightforward to predict.

Results

Taxonomic Composition of Oak Foliar Microbial Communities

Sequencing of the fungal ITS1 amplicon libraries yielded 297888 sequences, 259075 (86.97 %) of which passed the quality filtering procedures, and 251039 (84.27 %) of which were retained after the elimination of singleton sequences and after chimera filtering. The number of sequences per sample ranged from 1202 to 3725, with a mean of 2166 and a median of 2146. These sequences clustered into 1074 OTUs. Two OTUs assigned to *Q. robur* were excluded from the dataset. A putative taxonomic identification could be assigned to 747 of the remaining OTUs. Consistent with previous findings for foliar fungal communities [48–50], the taxonomically assigned OTUs were dominated by Ascomycota (492 OTUs, 55.1 % of the high-quality sequences), followed by Basidiomycota (252 OTUs, 10.5 %). One OTU was assigned to Glomeromycota and two to Zygomycota. The taxonomic composition of the foliar communities at the phylum and order levels is provided in the supplementary materials (Fig. S1).

Sequencing of the bacterial 16S amplicon pool yielded 30.5×10^6 sequences, 28.1×10^6 of which were oak chloroplast sequences that were filtered out. OTU clustering yielded 1507 OTUs, 820 of which were of bacterial origin. The number of bacterial sequences per sample ranged from 73 to 11706, with a mean of 1160 and a median of 668. Taxonomic assignment was possible for 816 of the bacterial OTUs. The bacterial phyla associated with the oak leaves were dominated by Proteobacteria (406 OTUs, 49 % of the high-quality bacterial sequences), composed of Alphaproteobacteria (205 OTUs, 25 %), Betaproteobacteria (96 OTUs, 12 %), Gammaproteobacteria (76 OTUs, 9 %), and Deltaproteobacteria (29 OTUs, 4 %). The other phyla identified were Firmicutes (175 OTUs, 21 %), Actinobacteria (114 OTUs, 14 %), Bacteroidetes (83 OTUs, 10 %), Acidobacteria (11 OTUs, 1 %), and others (31 OTUs, 4 %). The detailed taxonomic composition of the community at the phylum and order levels is provided in the supplementary materials (Fig. S2).

Comparison of Infection Levels Between Trees

As expected, the three trees differed significantly in both the percentage of the upper leaf area displaying symptoms (GLM; $F = 30.72$, df1 = 2, df2 = 113, $p < 0.001$) and the number of *E. alphitoides* reads (NBGLM; $\text{Chi}^2 = 91.62$, df = 2, $p < 0.001$). The percentage of the upper leaf area displaying symptoms of *E. alphitoides* infection and the number of *E. alphitoides* reads were significantly higher for the tree previously characterized as highly susceptible to powdery mildew than for the other two trees (Fig. 1).

These analyses revealed that *E. alphitoides* symptoms and reads were almost absent from the intermediately resistant tree and the strongly resistant tree. The percentage of the upper leaf area displaying symptoms was 12.9 % for the highly susceptible tree, 1.3 % for the tree with intermediate resistance, and 0.4 % for the highly resistant tree. The percentage of *E. alphitoides* reads was 5.4 % for the highly susceptible tree, 0.17 % for the tree with intermediate resistance, and 0.01 % for the highly resistant tree. In addition, *E. alphitoides* symptoms and reads showed large variations in abundance among leaves of the susceptible tree. The percentage of the upper leaf area displaying symptoms ranged from 0 to 80 %. The percentage of *E. alphitoides* reads ranged from 0 to 26.9 %. Therefore, we used the data collected for the susceptible tree to analyze the relationships between *E. alphitoides* and the residential microbial community. All analyses described below, including network inference, were performed on the data for the susceptible tree.

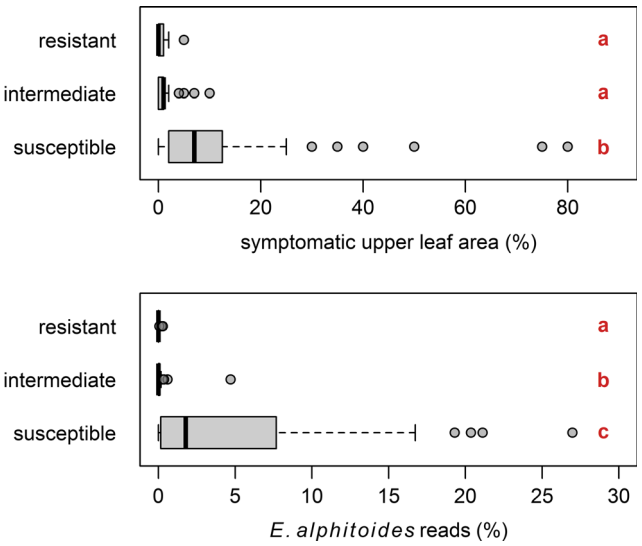

Fig. 1 Percentage of **a** the upper leaf area displaying symptoms and **b** reads assigned to the fungal pathogen *Erysiphe alphitoides* for three oak trees (*Quercus robur* L.) previously characterized as highly susceptible, intermediately resistant or highly resistant to powdery mildew on the basis of 5 years of visual observations. *Box and whisker plots* show the median percentage (*thick black line*), the quartiles (*boxes*), and the quartiles plus (*or minus*) one and a half times the interquartile range (*whiskers*). Outliers are shown as *circles*. *Letters* indicate the results of Tukey's test for pairwise comparisons. *Different letters* indicate significant differences between trees

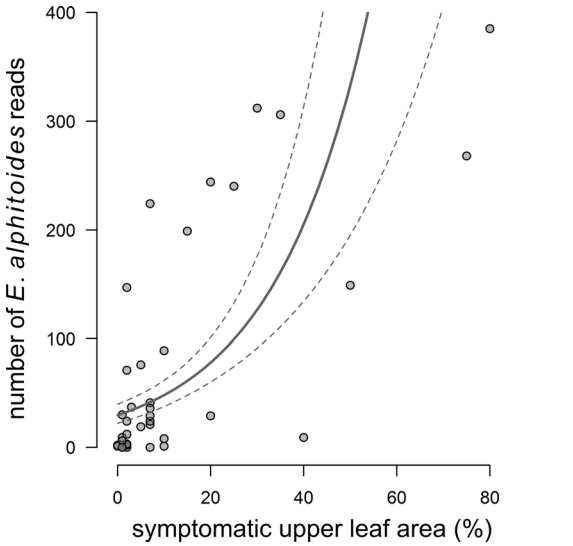

Fig. 2 Relationship between the percentage of the upper leaf area displaying symptoms and the number of reads assigned to the fungal pathogen *Erysiphe alphitoides*, across leaves sampled from an oak tree (*Quercus robur* L.) highly susceptible to *E. alphitoides*. The number of reads was obtained from a rarefied dataset with 1466 sequences per sample. The *solid gray line* shows the predictions of a negative binomial generalized linear model. *Dotted lines* indicate the standard errors of the predictions

Relationship Between the Level of Infection with *E. alphitoides* and the Composition of Foliar Microbial Communities

The analysis of leaves from the susceptible tree showed that the number of reads assigned to *E. alphitoides* increased significantly with the percentage of the upper leaf area displaying symptoms (NBGLM; $Chi^2 = 12.14$, df = 1, $p < 0.001$; Fig. 2). The number of reads assigned to *E. alphitoides* was therefore used as a proxy for the level of infection.

Principal coordinate analysis revealed that the level of infection with *E. alphitoides* was significantly related to fungal community composition. The percentage of *E. alphitoides* reads had a significant effect on *comp1* (GLM; $F = 17.21$, df1 = 1, df2 = 37, $p < 0.001$), but not on *comp2* (GLM; $F = 0.41$, df1 = 1, df2 = 37, $p = 0.52$). Differences in the percentage of *E. alphitoides* reads thus accounted for the differences in composition observed along the first axis of the PCoA (Fig. 3). Highly infected leaves had a higher abundance of OTU 3 (taxonomically unassigned at the species level). Leaves with a low abundance of *E. alphitoides* were separated into two groups differing in terms of their fungal community composition. The first group had a high abundance of OTU 1 (assigned to *Naevala minutissima*), OTU 10 (unassigned), and OTU 19 (unassigned). The second group had a high abundance of OTU 1278 (assigned to *Mycosphaerella punctiformis*).

Analyses of associations between fungal OTUs and leaf type (highly infected with *E. alphitoides versus* "uninfected") confirmed these results (Tab. S3). OTU 3 was significantly associated with highly infected leaves ($r = 0.38$, $p = 0.03$), whereas OTU 1278 and OTU 19 were significantly associated with uninfected leaves ($r = 0.39$, $p = 0.02$ and $r = 0.39$, $p = 0.009$, respectively). Moreover, OTU 26 (assigned to

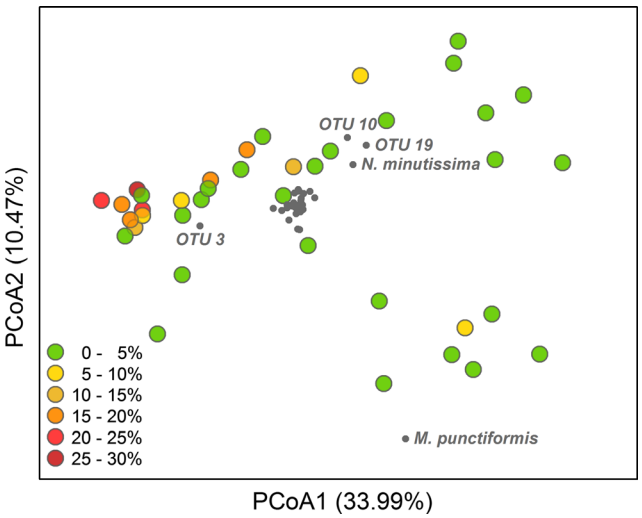

Fig. 3 Principal coordinates analysis showing Bray-Curtis dissimilarities in fungal community composition between the leaves of an oak tree (*Quercus robur* L.) highly susceptible to the fungal pathogen *Erysiphe alphitoides*. The *colors* indicate the level of infection with *E. alphitoides* for each leaf, measured as the percentage of reads assigned to *E. alphitoides*. The OTUs driving variation in fungal community composition are indicated in *dark gray*. *E. alphitoides* was considered to be external to the fungal community. The ordination was based on 100 rarefied datasets and was very robust to rarefaction

Taphrina carpini) and OTU 28 (assigned to *Sporobolomyces gracilis*) were also associated with infected ($r = 0.33$, $p = 0.05$) and uninfected leaves ($r = 0.47$, $p = 0.003$), respectively.

Similar to what was observed for the fungal community, the composition of the bacterial community was related to the level of infection with *E. alphitoides* (GLM; $F = 9.84$, df1 = 1, df2 = 37, $p = 0.003$ for *comp1*; $F = 0.12$, df1 = 1, df2 = 37, $p = 0.72$ for *comp2*). Analyses of associations between bacterial OTUs and leaf type (highly infected with *E. alphitoides versus* "uninfected") showed that 28 bacterial OTUs significantly increased in abundance with infection (Tab. S3). OTU 444 (assigned to *Methylobacterium* sp.) was most strongly associated with infected leaves ($r = 0.52$, $p = 0.001$). Nevertheless, principal coordinate analysis did not reveal clear differences in composition between infected and healthy leaves (Fig. S3). This result may be accounted for by the low rarefaction threshold used for analysis of the bacterial dataset (114 sequences per sample).

Putative Interactions between *E. alphitoides* and Other Members of the Foliar Community

The microbial interaction network inferred for the susceptible tree had 1099 edges, 65 % of which were positive. *E. alphitoides* was involved in 26 interactions in total (Fig. 4): 13 with fungal OTUs (6 positive, 7 negative) and 13 with bacterial OTUs (6 positive, 7 negative). The list of these OTUs is provided in Table 1, together with their taxonomic assignments. Corresponding sequences are available in the supplementary materials (Text S1 and S2). The majority of the fungal species highlighted in ordination and association analyses were considered likely to interact directly with *E. alphitoides* (Tab. S3). OTU 1 (assigned to *N. minutissima*), OTU 10, OTU19 (both taxonomically unassigned at the species level), OTU 28 (assigned to *Sporobolomyces gracilis*) and OTU 1278 (assigned to *Mycosphaerella punctiformis*) were linked to *E. alphitoides* by negative edges. OTU 26 (assigned to *Taphrina carpini*) was linked to *E. alphitoides* through a positive edge. The network inference highlighted seven other fungal OTUs likely to interact directly with *E. alphitoides*. Both OTU 2 (also assigned to *M. punctiformis*) and OTU 15 (assigned to *Monochaetia kansensis*) were linked negatively to *E. alphitoides*. The network inference also revealed that among the 28 bacterial OTUs that significantly increase in abundance with infection, only 5 were likely to interact directly with *E. alphitoides*. These 5 OTUs were linked positively to *E. alphitoides* in the network (Tab. S3).

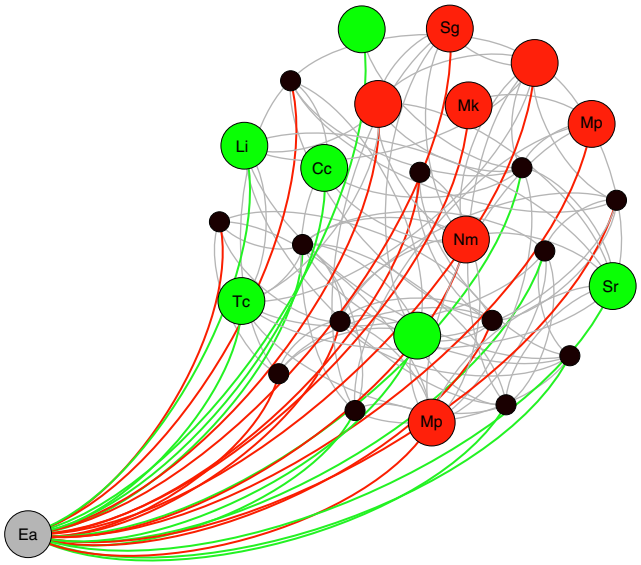

Fig. 4 Model of the pathobiome of *Erysiphe alphitoides* on oak leaves (*Quercus robur* L.). Network nodes correspond to microbial OTUs. OTUs are linked if they are likely to interact together through direct ecological interactions, according to the results of a Bayesian model of network inference. The *large gray node* corresponds to *E. alphitoides* (*Ea*). *Small black nodes* correspond to bacterial OTUs. The *large green nodes* are fungal OTUs positively associated with Ea. The *large red nodes* are fungal OTUs negatively associated with Ea. Interactions between Ea and other OTUs are represented in *green* when the OTUs are positively associated and in *red* when they tend to exclude each other. Interactions between the interacting partners of Ea are shown in *gray*. The names of the fungal OTUs that could be assigned to species level are indicated. *Cc*: *Cladosporium cladosporioides*; *Li*: *Lalaria inositophila*; *Nm*: *Naevala minutissima*; *Mp*: *Mycosphaerella punctiformis*; *Mk*: *Monochaetia kansensis*; *Tc*: *Taphrina carpini*; *Sg*: *Sporobolomyces gracilis*; *Sr*: *Sporobolomyces roseus*

Discussion

The pathobiome concept has been defined in the context of microbial community interactions [5]. It can be viewed as a subset of the microbiome of a host, centered on a pathogen species. The microbiome corresponds to the totality of microbes (bacteria, archaea, and fungi) in a given environment and the totality of functions performed by this microbiota [51]. The pathobiome can thus be defined as the totality of microbes interacting with a given pathogen species and their influence on pathogenesis. We showed here that the pathobiome can be studied by combining metabarcoding and network inference analyses.

There are several prerequisites for studies of the pathobiome of a given pathogen by combining metabarcoding and network inference. First, there should be a significant relationship between the abundance of a microbial species and the number of sequences assigned to it. In particular, there should be a significant relationship between the level of infection with the pathogen and the number of sequences assigned to it. This condition was met for *E. alphitoides*, the causal agent of oak powdery mildew [22, 23], at both the leaf and tree levels. These results are consistent with those recently obtained by Sapkota et al. [52] for two foliar diseases of cereals. Another prerequisite is good preservation of the composition of the microbial community during tissue storage before

Table 1 Taxonomic assignment of the 26 operational taxonomic units (OTUs) potentially interacting with *Erysiphe alphitoides* (Ea) according to the inferred microbial network. The sign of the interaction indicates whether the OTUs are positively or negatively associated to *E. alphitoides*. Taxonomic assignments were performed by using the RDP Classifier and by BLAST analysis of OTU representative sequences against GenBank. Coverage is the percentage of the query length covered by the alignment. Similarity is the percentage identity over the alignment

Phylum	OTU	Interaction with *Ea*	Taxonomic classification in RDP (confidence > 80%)	Closest match in GenBank	Coverage (%)	Similarity (%)	Putative species/genus
Fungi	19	−0.244	Fungi (99 %)	–	–	–	NA
	10	−0.194	Ascomycota (83 %)	–	–	–	NA
	1	−0.179	Ascomycota (100 %), Helotiales (87 %)	AY853228.1	100	100	*Naevala minutissima*
	1278	−0.179	Ascomycota (100 %)	KC339234.1	100	97	*Mycosphaerella punctiformis*
	28	−0.161	Basidiomycota (100 %), Sporidiobolales (100 %), *Sporobolomyces gracilis* (99 %)	KJ706995.1	100	99	*Sporobolomyces gracilis*
	15	−0.145	Ascomycota (100 %), Xylariales (100 %), *Monochaetia kansensis* (100 %)	KC345691.1	100	100	*Monochaetia kansensis*
	2	−0.139	Ascomycota (100 %)	KC339234.1	100	100	*Mycosphaerella punctiformis*
	1567	0.124	Basidiomycota (100 %), Cystofilobasidiales (100 %)	–	–	–	NA
	9	0.146	Ascomycota (100 %), Capnodiales (100 %), *Davidiella tassiana* (100 %)	KP836326.1	100	100	*Cladosporium cladosporioides*
	25	0.178	Basidiomycota (90 %)	–	–	–	NA
	23	0.181	Basidiomycota (100 %)	HG008766.1	100	99	*Sporobolomyces roseus*
	20	0.241	Ascomycota (100 %), Taphrinales (100 %), *Lalaria inositophila* (100 %)	AY239214.1	100	100	*Lalaria inositophila*
	26	0.265	Ascomycota (100 %), Taphrinales (100 %), *Lalaria carpini* (100 %)	AF492085.1	100	100	*Taphrina carpini*
Bacteria	625	−0.243	Betaproteobacteria (99 %), Burkholderiales (99 %)	KR265624.1	97	97	*Acidovorax* sp.
	27	−0.221	Betaproteobacteria (99 %), Burkholderiales (92 %), Ralstonia (92 %)	JN545036.1	100	98	*Ralstonia* sp.
	49	−0.204	Gammaproteobacteria (99 %)	LN829899.2	100	99	*Arsenophonus* sp.
	63	−0.195	Alphaproteobacteria(94 %), Rhizobiales (94 %), Methylobacterium (94 %)	JX993414.1	97	98	*Methylobacterium* sp.
	90	−0.187	Proteobacteria (84 %)	KM253240.1	97	94	*Burkholderia* sp.
	112	−0.175	Betaproteobacteria (97 %), Burkholderiales (89 %)	KM253240.1	97	98	*Burkholderia* sp.
	87	−0.165	Bacilli (96 %), Bacillales (91 %), Staphylococcus (83 %)	HQ179145.1	97	100	*Staphylococcus* sp.
	31	0.144	Alphaproteobacteria (90 %)	JX448502.1	96	99	*Sphingomonas* sp.
	444	0.151	Alphaproteobacteria (91 %), Rhizobiales (91 %)	KR265692.1	97	98	*Methylobacterium* sp.
	1191	0.186	Bacteroidetes (85 %)	KM203869.1	94	97	*Hymenobacter* sp.
	42	0.19	Alphaproteobacteria (94 %), Rhizobiales (94 %)	KF681060.1	97	98	*Methylobacterium* sp.
	33	0.2	Actinobacteria (95 %), Actinomycetales (95 %), Curtobacterium (89 %)	KR181798.1	97	99	*Frondihabitans* sp.
	20	0.21	Alphaproteobacteria (96 %), Rhizobiales (96 %), Methylobacterium (94 %)	AB698681.1	97	98	*Methylobacterium* sp.

NA non-available

the analysis. Our results indicate that the storage of oak leaves in silica gel for a period of 2 weeks does not bias the composition of the foliar fungal community composition inferred by 454-pyrosequencing. However, these results contrast with those obtained by U'Ren et al. [53] for moss and lichen species. Finally, a last prerequisite is the availability of network

inference methods. Here, we used the Bayesian method of network inference developed by Schwaller et al. [20] to highlight the most likely microbial interactions in the habitat formed by oak leaves (*Q. robur* L.).

Against expectation, our results suggested that mutualism, facilitation, and commensalism may dominate microbial interactions in oak leaves. More than half of the edges in the microbial interaction network were indeed positive. These results contrast with other findings showing that competition is by far the most frequent outcome in microbial species interactions [54, 55]. This high proportion of positive microbial interactions may be accounted for by the fact that our analyses were based on a snapshot of the microbial communities, taken about 3 months after leaf unfolding. Many competitive interactions may have occurred before this time point. The weaker competitors may already have been excluded, tipping the scales towards positive interactions.

Our results also revealed that the composition of the fungal community of oak leaves changed markedly with the level of *E. alphitoides* infection. The composition of the phyllosphere yeast community, in particular, varied significantly with infection. The yeast species *T. carpini*, for example, was associated with highly infected leaves, whereas *S. gracilis* was found more frequently on leaves with a low abundance of *E. alphitoides*. The composition of the bacterial community also changed significantly with the level of *E. alphitoides* infection, but changes were less clear-cut than that of fungi. According to the inferred microbial network, several direct interactions between *E. alphitoides* and bacteria may however occur. The positive interactions between bacterial OTUs and the fungal pathogen may be accounted for by endosymbiosis [56]. They may also be accounted for by commensalism. For instance, bacteria may use dead hyphae as a source of nutrients. Bacteria may also facilitate fungal infection [57] because they benefit from the changes in plant metabolism induced by the fungal pathogen.

In addition to phyllosphere yeasts and bacteria, several fungal endophytes differed significantly in abundance between infected and uninfected leaves. *M. punctiformis* was one of them. This species colonizes living oak leaves as an endophyte, without causing symptoms, and then sporulates on senescent leaves [58]. According to the microbial interaction network, there may be a direct, antagonistic ecological interaction between *M. punctiformis* and *E. alphitoides*. This finding suggests that *M. punctiformis* could protect oak leaves against powdery mildew. *E. alphitoides* is an obligate parasite. In vivo experiments are therefore required to validate the antagonistic relationship between the two species and to decipher the mechanism underlying the interaction. According to our results, *M. kansensis* is another foliar endophyte that might compete with *E. alphitoides*. This fungus has already been observed on various *Quercus* species, including pedunculate oak [59], and it is known to produce various bioactive compounds [60]. By contrast, the ubiquitous foliar endophyte *Cladosporium cladosporioides* was positively linked to *E. alphitoides* in the microbial interaction network. This endophyte is considered to be a weakness parasite, becoming virulent only when the host plant is weakened by stress. Its abundance has been shown to be higher in declining oak trees than in healthy trees [61]. Our results suggest that leaf infection with *E. alphitoides* might favor this species.

In conclusion, our results show that complex networks of microbe-microbe interactions occur on oak leaves. Network inference highlighted 13 bacterial OTUs and 13 fungal OTUs likely to interact directly with the *E. alphitoides*, the causal agent of oak powdery mildew. Two foliar endophytic species—*M. punctiformis* and *M. kansensis*—were highlighted as potential antagonists of *E. alphitoides*. Several phyllosphere yeasts were also found to be likely to interact directly with *E. alphitoides*. Controlled inoculations will be required to validate these potential interactions. Studies of the temporal dynamics of microbial networks during the course of infection also appear to be a promising avenue of research likely to provide deeper insight into the ecology of this disease and to improve its biological control. The biological control of forest diseases remains rare [62]. We show here that combining metagenomics and network inference may foster this method of forest protection, by highlighting potential antagonistic interactions between pathogens and other microorganisms.

Acknowledgments We thank Xavier Capdevielle, Olivier Fabreguettes, Laure Villate, and Martine Martin-Clotté (INRA, BioGeCo) for technical assistance and advice during preliminary experiments and during the course of the study. We also thank Franck Salin, Thibaut Decourcelle, Adline Delcamp, and Christophe Hubert (CGFB, Bordeaux) for sequencing the samples. The costs of sampling and sequencing were covered by the AIP Bioressource METAPHORE. Computing facilities were provided by the MCIA (*Mésocentre de Calcul Intensif Aquitain*) of the *Université de Pau et des Pays de l'Adour*. BJ received a grant from the French Ministry of Research and Education (MENRT no. 2011/AF/57). We thank Cindy E. Morris for helpful discussions about the phyllosphere. We thank Sarah Ouadah and Stéphane Robin for supervising the network analyses. We thank Marie-Laure Desprez-Loustau, Arndt Hampe, Samantha Yeo, and David Bohan and four anonymous reviewers for their very helpful comments. We also thank Julie Sappa from Alex Edelman & Associates for English language revision.

References

1. Turner TR, James EK, Poole PS (2013) The plant microbiome. Genome Biol 14:209. doi:10.1186/gb-2013-14-6-209
2. Faust K, Raes J (2012) Microbial interactions: from networks to models. Nat Rev Microbiol 10:538–550. doi:10.1038/nrmicro2832
3. Frey-Klett P, Burlinson P, Deveau A et al (2011) Bacterial-fungal interactions: hyphens between agricultural, clinical, environmental, and food microbiologists. Microbiol Mol Biol Rev 75:583–609. doi:10.1128/MMBR.00020-11

4. Kemen E (2014) Microbe-microbe interactions determine oomycete and fungal host colonization. Curr Opin Plant Biol 20: 75–81. doi:10.1016/j.pbi.2014.04.005
5. Vayssier-Taussat M, Albina E, Citti C et al (2014) Shifting the paradigm from pathogens to pathobiome: new concepts in the light of meta-omics. Front Cell Infect Microbiol 4:29. doi:10.3389/fcimb.2014.00029
6. Thiele I, Heinken A, Fleming RMT (2013) A systems biology approach to studying the role of microbes in human health. Curr Opin Biotechnol 24:4–12. doi:10.1016/j.copbio.2012.10.001
7. Gaggia F, Mattarelli P, Biavati B (2010) Probiotics and prebiotics in animal feeding for safe food production. Int J Food Microbiol 141: S15–S28. doi:10.1016/j.ijfoodmicro.2010.02.031
8. Clemente JC, Ursell LK, Parfrey LW, Knight R (2012) The impact of the gut microbiota on human health: an integrative view. Cell 148:1258–1270. doi:10.1016/j.cell.2012.01.035
9. Ursell LK, Van Treuren W, Metcalf JL et al (2013) Replenishing our defensive microbes. Bioessays 35:810–817. doi:10.1002/bies.201300018
10. Berlec A (2012) Novel techniques and findings in the study of plant microbiota: search for plant probiotics. Plant Sci 193–194:96–102. doi:10.1016/j.plantsci.2012.05.010
11. Newton AC, Gravouil C, Fountaine JM (2010) Managing the ecology of foliar pathogens: ecological tolerance in crops. Ann Appl Biol 157:343–359. doi:10.1111/j.1744-7348.2010.00437.x
12. Vacher C, Tamaddoni-Nezhad A, Kamenova S et al (2016) Learning ecological network from NGS data. Adv Ecol Res 54: 1–39. doi:10.1016/bs.aecr.2015.10.004
13. Agler MT, Ruhe J, Kroll S et al (2016) Microbial hub taxa link host and abiotic factors to plant microbiome variation. PLoS Biol 14, e1002352. doi:10.1371/journal.pbio.1002352
14. Okuyama T, Holland JNN (2008) Network structural properties mediate the stability of mutualistic communities. Ecol Lett 11: 208–216. doi:10.1111/j.1461-0248.2007.01137.x
15. Thébault E, Fontaine C (2010) Stability of ecological communities and the architecture of mutualistic and trophic networks. Science 329:853–856. doi:10.1126/science.1188321
16. Hui C, Richardson DM, Landi P et al (2016) Defining invasiveness and invasibility in ecological networks. Biol Invasions, online. doi:10.1007/s10530-016-1076-7
17. Kurtz ZD, Mueller CL, Miraldi ER et al (2015) Sparse and compositionally robust inference of microbial ecological networks. PLoS Comput Biol 11, e1004226. doi:10.1371/journal.pcbi.1004226
18. Friedman J, Alm EJ (2012) Inferring correlation networks from genomic survey data. PLoS Comput Biol 8, e1002687. doi:10.1371/journal.pcbi.1002687
19. Deng Y, Jiang Y-H, Yang Y et al (2012) Molecular ecological network analyses. BMC Bioinformatics 13:113. doi:10.1186/1471-2105-13-113
20. Schwaller L, Robin S, Stumpf M (2015) Bayesian Inference of Graphical Model Structures Using Trees. arXiv:1504.02723
21. Schwaller L (2015) saturnin: Spanning Trees Used for Network Inference. R Package version 1.0. http://CRAN.R-project.org/package=saturnin
22. Mougou A, Dutech C, Desprez-Loustau M-L (2008) New insights into the identity and origin of the causal agent of oak powdery mildew in Europe. For Pathol 38:275–287. doi:10.1111/j.1439-0329.2008.00544.x
23. Mougou-Hamdane A, Giresse X, Dutech C, Desprez-Loustau M-L (2010) Spatial distribution of lineages of oak powdery mildew fungi in France, using quick molecular detection methods. Ann For Sci 67:212
24. Glawe DA (2008) The powdery mildews: a review of the world's most familiar (yet poorly known) plant pathogens. Annu Rev Phytopathol 46:27–51. doi:10.1146/annurev.phyto.46.081407.104740
25. Kiss L (2003) A review of fungal antagonists of powdery mildews and their potential as biocontrol agents. Pest Manag Sci 59:475–483. doi:10.1002/ps.689
26. Copolovici L, Väärtnõu F, Estrada MP, Niinemets Ü (2015) Oak powdery mildew (*Erysiphe alphitoides*) induced volatile emissions scale with the degree of infection in *Quercus robur*. Tree Physiol 34:1399–1410. doi:10.1093/treephys/tpu091.Oak
27. Hajji M, Dreyer E, Marçais B (2009) Impact of *Erysiphe alphitoides* on transpiration and photosynthesis in *Quercus robur* leaves. Eur J Plant Pathol 125:63–72. doi:10.1007/s10658-009-9458-7
28. Scotti-Saintagne C, Bodénès C, Barreneche T et al (2004) Detection of quantitative trait loci controlling bud burst and height growth in *Quercus robur* L. Theor Appl Genet 109:1648–1659. doi:10.1007/s00122-004-1789-3
29. Schoch CL, Seifert KA, Huhndorf S et al (2012) Nuclear ribosomal internal transcribed spacer (ITS) region as a universal DNA barcode marker for Fungi. Proc Natl Acad Sci 109:6241–6246. doi:10.1073/pnas.1117018109
30. Gardes M, Bruns TD (1993) ITS primers with enhanced specificity for basidiomycetes - application to the identification of mycorrhizae and rusts. Mol Ecol 2:113–118
31. White T, Bruns T, Lee S, Taylor J (1990) Amplification and direct sequencing of fungal ribosomal RNA genes for phylogenetics. In: Innis MA, Gelfand DH, Sninsky JJ, White TJ (eds) PCR protocols: a guide to methods and applications. Academic Press, Inc, New York, N.Y, pp 315–322
32. Gloor GB, Hummelen R, Macklaim JM et al (2010) Microbiome profiling by Illumina sequencing of combinatorial sequence-tagged PCR products. PLoS One 5, e15406. doi:10.1371/journal.pone.0015406
33. Huse SM, Dethlefsen L, Huber JA et al (2008) Exploring microbial diversity and taxonomy using SSU rRNA hypervariable tag sequencing. PLoS Genet 4, e1000255. doi:10.1371/journal.pgen.1000255
34. Caporaso JG, Kuczynski J, Stombaugh J et al (2010) QIIME allows analysis of high-throughput community sequencing data. Nat Methods 7:335–336. doi:10.1038/nmeth.f.303
35. Nilsson RH, Veldre V, Hartmann M et al (2010) An open source software package for automated extraction of ITS1 and ITS2 from fungal ITS sequences for use in high-throughput community assays and molecular ecology. Fungal Ecol 3:284–287. doi:10.1016/j.funeco.2010.05.002
36. Edgar RC (2013) UPARSE: highly accurate OTU sequences from microbial amplicon reads. Nat Methods 10:996–998. doi:10.1038/nmeth.2604
37. Edgar RC (2010) Search and clustering orders of magnitude faster than BLAST. Bioinformatics 26:2460–2461. doi:10.1093/bioinformatics/btq461
38. Nilsson RH, Kristiansson E, Ryberg M, Hallenberg N (2008) Intraspecific ITS Variability in the Kingdom Fungi as Expressed in the International Sequence Databases and Its Implications for Molecular Species Identification. Evol Bioinforma 4:193–201
39. Nilsson RH, Bok G, Ryberg M et al (2009) A software pipeline for processing and identification of fungal ITS sequences. Source Code Biol Med 4:1. doi:10.1186/1751-0473-4-1
40. Altschul SF, Gish W, Miller W et al (1990) Basic Local Alignment Search Tool. J Mol Biol 215:403–410
41. Wang Q, Garrity GM, Tiedje JM, Cole JR (2007) Naive Bayesian classifier for rapid assignment of rRNA sequences into the new bacterial taxonomy. Appl Environ Microbiol 73:5261–5267. doi:10.1128/AEM.00062-07
42. Abarenkov K, Nilsson RH, Larsson KH et al (2010) The UNITE database for molecular identification of fungi—recent updates and future perspectives. New Phytol 186:281–285

43. Masella AP, Bartram AK, Truszkowski JM et al (2012) PANDAseq: paired-end assembler for illumina sequences. BMC Bioinformatics 13:31. doi:10.1186/1471-2105-13-31
44. Bengtsson J, Eriksson KM, Hartmann M et al (2011) Metaxa: a software tool for automated detection and discrimination among ribosomal small subunit (12S/16S/18S) sequences of archaea, bacteria, eukaryotes, mitochondria, and chloroplasts in metagenomes and environmental sequencing datasets. Antonie Van Leeuwenhoek Int J Gen Mol Microbiol 100:471–475. doi:10.1007/s10482-011-9598-6
45. R_Core_Team (2013) R: A Language and Environment for Statistical Computing. http://www.R-project.org.
46. McMurdie PJ, Holmes S (2014) Waste not, want not: why rarefying microbiome data is inadmissible. PLoS Comput Biol 10, e1003531. doi:10.1371/journal.pcbi.1003531
47. Bastian M, Heymann S (2009) Gephi : An Open Source Software for Exploring and Manipulating Networks. Int. AAAI Conf. Weblogs Soc. Media.
48. Jumpponen A, Jones KL (2009) Massively parallel 454 sequencing indicates hyperdiverse fungal communities in temperate *Quercus macrocarpa* phyllosphere. New Phytol 184:438–448. doi:10.1111/j.1469-8137.2009.02990.x
49. Cordier T, Robin C, Capdevielle X et al (2012) Spatial variability of phyllosphere fungal assemblages: genetic distance predominates over geographic distance in a European beech stand (*Fagus sylvatica*). Fungal Ecol 5:509–520. doi:10.1016/j.funeco.2011.12.004
50. Douanla-Meli C, Langer E, Talontsi Mouafo F (2013) Fungal endophyte diversity and community patterns in healthy and yellowing leaves of Citrus limon. Fungal Ecol 6:212–222. doi:10.1016/j.funeco.2013.01.004
51. Schlaeppi K, Bulgarelli D (2015) The plant microbiome at work. MPMI 28:212–217
52. Sapkota R, Knorr K, Jørgensen LN et al (2015) Host genotype is an important determinant of the cereal phyllosphere mycobiome. New Phytol 207:1134–1144
53. U'Ren JM, Riddle JM, Monacell JT et al (2014) Tissue storage and primer selection influence pyrosequencing-based inferences of diversity and community composition of endolichenic and endophytic fungi. Mol Ecol Resour 14:1032–1048. doi:10.1111/1755-0998.12252
54. Hibbing ME, Fuqua C, Parsek MR, Peterson SB (2010) Bacterial competition: surviving and thriving in the microbial jungle. Nat Rev Microbiol 8:15–25. doi:10.1038/nrmicro2259
55. Foster KR, Bell T (2012) Competition, not cooperation, dominates interactions among culturable microbial species. Curr Biol 22:1845–1850. doi:10.1016/j.cub.2012.08.005
56. Hoffman MT, Arnold AE (2010) Diverse bacteria inhabit living hyphae of phylogenetically diverse fungal endophytes. Appl Environ Microbiol 76:4063–4075. doi:10.1128/AEM.02928-09
57. Venturi V, da Silva DP (2012) Incoming pathogens team up with harmless "resident" bacteria. Trends Microbiol 20:160–164. doi:10.1016/j.tim.2012.02.003
58. Verkley GJM, Crous PW, Groenewald JZ et al (2004) *Mycosphaerella punctiformis* revisited: morphology, phylogeny, and epitypification of the type species of the genus Mycosphaerella (Dothideales, Ascomycota). Mycol Res 108:1271–1282. doi:10.1017/S0953756204001054
59. Gennaro M, Gonthier P, Nicolotti G (2003) Fungal endophytic communities in healthy and declining *Quercus robur* L. and *Q. cerris* L. trees in Northern Italy. J Phytopathol 151:529–534. doi:10.1046/j.1439-0434.2003.00763.x
60. Yogeswari S, Ramalakshmi S, Neelavathy R, Muthumary J (2012) Identification and comparative studies of different volatile fractions from *Monochaetia kansensis* by GCMS. Glob J Pharmacol 6:65–71
61. Ragazzi A, Moricca S, Capretti P et al (2001) Endophytic fungi in Quercus cerris: isolation frequency in relation to phenological phase, tree health and the organ affected. Phytopathol Mediterr 40:165–171
62. Witzell J, Martin JA, Blumenstein K (2014) Ecological Aspects of Endophyte-Based Biocontrol of Forest Diseases. In Advances in Endophytic Research, eds. VC Verma, AC Gange, pp. 321–33